Inorganic Chemistry

Article

pubs.acs.org/IC

Detailed Electrochemical Studies of the Tetraruthenium Polyoxometalate Water Oxidation Catalyst in Acidic Media: Identification of an Extended Oxidation Series using Fourier Transformed Alternating Current Voltammetry

Chong-Yong Lee,[†] Si-Xuan Guo,[†] Aidan F. Murphy,[†,‡] Timothy McCormac,[‡] Jie Zhang,*[,†] Alan M. Bond,*[,†] Guibo Zhu,[§] Craig L. Hill,[§] and Yurii V. Geletii*[,§]

[†]School of Chemistry, Monash University, Clayton, Victoria 3800, Australia

[‡]Dundalk Institute of Technology, Dundalk Co. Louth, Ireland

[§]Department of Chemistry, Emory University, Atlanta, Georgia 30322, United States

ABSTRACT: The electrochemistry of the water oxidation catalyst, $Rb_8K_2[\{Ru_4O_4(OH)_2(H_2O)_4\}(\gamma\text{-}SiW_{10}O_{36})_2]$ (Rb_8K_2-**1**(0)) has been studied in the presence and absence of potassium cations in both hydrochloric and sulfuric acid solutions by transient direct current (dc) cyclic voltammetry, a steady state dc method in the rotating disk configuration and the kinetically sensitive technique of Fourier transformed large-amplitude alternating current (ac) voltammetry. In acidic media, the presence of potassium ions affects the kinetics (apparent rate of electron transfer) and thermodynamics (reversible potentials) of the eight processes (A′/A to H/H′) that are readily detected under dc voltammetric conditions. The six most positive processes (A′/A to F/F′), each involve a one electron ruthenium based charge transfer step (A′/A, B′/B are $Ru^{IV/V}$ oxidation and C/C′ to F/F′ are $Ru^{IV/III}$ reduction). The apparent rate of electron transfer of the ruthenium centers in sulfuric acid is higher than in hydrochloric acid. The addition of potassium cations increases the apparent rates and gives rise to a small shift of reversible potential. Simulations of the Fourier transformed ac voltammetry method show that the B′/B, E/E′, and F/F′ processes are quasi-reversible, while the others are close to reversible. A third $Ru^{IV/V}$ oxidation process is observed just prior to the positive potential limit via dc methods. Importantly, the ability of the higher harmonic components of the ac method to discriminate against the irreversible background solvent process allows this (process I) as well as an additional fourth reversible ruthenium based process (J) to be readily identified. The steady-state rotating disk electrode (RDE) method confirmed that all four Ru-centers in Rb_8K_2-**1**(0) are in oxidation state IV. The dc and ac data indicate that reversible potentials of the four ruthenium centers are evenly spaced, which may be relevant to understanding of the water oxidation electrocatalysis. A profound effect of the potassium cation is observed for the one-electron transfer process (G/G′) assigned to $Ru^{III/II}$ reduction and the multiple electron transfer reduction process (H/H′) that arise from the tungstate polyoxometalate framework. A significant shift of $E^{\circ\prime}$ to a more positive potential value for process H/H′ was observed on removal of K^+ (~100 mV in H_2SO_4 and ~50 mV in HCl).

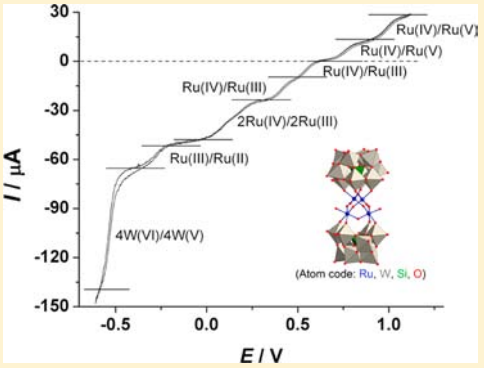

INTRODUCTION

Ruthenium transition metal based molecular catalysts are widely developed.[1] Although ruthenium is more expensive than many other transition metals, it is regarded as a benchmark material for the water splitting application.[2] The drawback of molecular catalysts that employ organic ligands is that they have a tendency to degrade via the intermediates generated in the oxidative water splitting processes, thereby compromising the long-term stability of the catalyst.[3−6] To minimize this problem, the design of ruthenium based molecular catalysts containing only inorganic ligands is highly desirable. Polyoxometalates offer access to an architecture where all the inorganic materials contain multiple ruthenium centers in accordance with the requirements needed to meet the uphill task of an overall four-electron transfer needed to oxidize water. Recent reports of a tetraruthenium polyoxometalate, $Rb_8K_2[\{Ru_4O_4(OH)_2(H_2O)_4\}(\gamma\text{-}SiW_{10}O_{36})_2]$ (abbreviation Rb_8K_2-**1**(0)),[7,8] and the same materials based on Li^+ or Cs^+ cations[9,10] not only meet the criteria of a totally inorganic and robust ligand system, but also give rise to excellent water oxidation activity.

Adapted from nature, stabilization of adjacent ruthenium transition metal centers in Rb_8K_2-**1**(0) was achieved in these water splitting catalysts through multiple μ-hydroxo/oxo bridging units that form a catalytically active tetraruthenium-

Received: June 27, 2012
Published: October 23, 2012

   dx.doi.org/10.1021/ic301370y | *Inorg. Chem.* 2012, 51, 11521−11532

(IV)-μ-oxo core which is embedded by the polyoxometalate framework based on γ-decatungstosilicate (γ-$SiW_{10}O_{36}$). The properties of this Ru-polyoxometalate have been probed via many analytical techniques. The main aim of these studies has been to understand the multiple electron transfer and possible proton coupled electron transfer reactions derived from tetraruthenium(IV)-μ-oxo core and their relationship to water oxidation. Indeed, understanding of the complex four-electron, four-proton reaction is one of the most important challenges in the development of artificial photosynthesis systems that can store chemical energy via sunlight.[11] Electrochemistry provides one of the most straightforward and informative approaches in elucidating details of the redox chemistry relevant to the kinetics and thermodynamics of ruthenium in multiple oxidation states.

The electrochemistry of polyoxometalate anions is known to depend on parameters such as solvent medium, supporting electrolyte, proton concentration, and the presence of cations, all of which have been reported to significantly affect electron-transfer and catalytic properties.[12−20] A brief study on the influence of alkali metal cations such as lithium, sodium and potassium on Rb_8K_2-**1**(0) indicates the latter has the most pronounced effect.[8] In this study, we now quantitatively probe the electrochemistry of Rb_8K_2-**1**(0) in acid media in the presence and absence of potassium ions, using direct current (dc) cyclic, rotating disk electrode, and the large-amplitude alternating current (ac) voltammetric methods. Both the ruthenium and tungsten redox active centers are investigated. To maintain well-defined voltammetry, we focus on acidic conditions. Ultimately, equally detailed studies will be needed to elucidate the redox chemistry in the neutral to alkaline pH region.

With the highly kinetically sensitive technique of large-amplitude ac voltammetry,[21] comparisons of experimental data with simulations have been employed to quantify the kinetics of the redox processes. The background current rejection feature available in the higher harmonics of this technique is extremely useful for evaluation of the faradaic processes.[22−24] In contrast, this very high molecular weight complex gives relatively unfavorable faradaic to background current under dc conditions. The ac method has been previously applied to access the underlying Ru^{II} to Ru^{VII} faradaic process associated with the electrochemistry of RuO_2 which is dominated by a very large background pseudocapacitance current.[25] In addition to the oxidation and reduction of the tetra-ruthenium center, the investigation is extended to include the polyoxometalate framework of didecatungstosilicate ($SiW_{10}O_{36}$) that has not yet been addressed in detail.

EXPERIMENTAL SECTION

Chemicals. Rb_8K_2-**1**(0) was synthesized using the procedure described elsewhere.[7] This complex is synthesized under air and is stable in water under air for at least 6 months. KCl, K_2SO_4, and HCl (AR grade, BDH) and H_2SO_4 (AR grade, Univar) were used as supplied by the manufacturers. Deionized water from a Milli-Q-MilliRho purification system (resistivity >18 MΩ × cm) was used to prepare all aqueous electrolyte solutions.

Apparatus and Procedures. Conventional dc cyclic voltammetric and rotating disk electrode experiments were carried out using a Bioanalytical Systems (BAS West Lafayette, Indiana) Model 100B or a CHI 700D electrochemical workstation (CH Instruments, Austin, Texas, U.S.A.). A BAS RDE-2 accessory connected to the BAS 100 B electrochemical workstation or a Rotating Ring Disk Electrode Rotator (RRDE-3A) (ALS Co., Japan) connected to the CHI 700D electrochemical workstation was used for the RDE experiments. Large amplitude Fourier transformed ac voltammetric methods were undertaken with a home-built apparatus described elsewhere,[19] using an applied ac perturbation, superimposed onto the dc ramp, of amplitude 80 mV and frequency 9.02 Hz. The total current measured by this waveform was then subjected to Fourier transformation that separates the current into a number of components, which are displayed as the power spectrum. After selection of the frequency band of interest and filtering out the unrequired frequencies, inverse Fourier Transformation was used to generate the required dc or ac harmonic current component. In this study, the ac harmonics are presented for convenience in an "envelope" format rather than the full current−time version.[19]

An all-glass three-electrode cell was employed in electrochemical measurements. The glassy carbon working electrode (geometric area of 0.07 cm^2) was purchased from BAS. Prior to use in voltammetric experiments, both working electrodes were polished with an aqueous 0.3 μm alumina suspension on a polishing cloth (Buehler), rinsed with water, then sonicated to remove excess alumina, before a final rinse with water and drying in nitrogen. Ag/AgCl (3 M NaCl) was employed as the reference electrode and platinum wire as the auxiliary electrode.

All voltammetric experiments were undertaken at 20 ± 1 °C, and the solutions were degassed with nitrogen for at least 5 min prior to commencing the measurements.

Thin-layer spectroelectrochemistry was carried out using the SEC-2F spectroelectrochemical flow cell with ITO working electrode (ALS Co., Japan) attached to the USB2000+VIS-NIR fiber optic spectrometer (Ocean Optics, U.S.A.).

The pH was measured with a Metrohm 744 pH meter, equipped with a Metrohm 6.2306.020 glass electrode (Metrohm, Herisau, Switzerland). Standard buffer solutions for the calibration of the pH meter were provided by Metrohm (Metrohm, Herisau, Switzerland): no. 6.2307.100 (pH 3.99 at 20 °C) and no. 6.2307.110 (pH 7.02 at 20 °C). The built-in reference electrode that is used with the Metrohm glass electrode is Ag/AgCl in 3 M KCl. The latter minimizes junction potentials in both the reference and the analyte solutions. The accuracy of calibration at very low pH was controlled by using a standard buffer solution pH 1.0 (at 20 °C) purchased from Sigma-Aldrich (U.S.A.).

Digital Simulations of AC Voltammetry. AC cyclic voltammetric results were simulated using MECSim (Monash Electrochemical Simulator), an internally developed software program. This simulation package is written in Fortran 77 and is based on the matrix formulation outlined in our previous publications.[26,27] Output for the dc simulations was obtained by using a zero amplitude (ΔE = 0 V) for the ac component. Simulations of dc cyclic voltammograms using MECSim was routinely compared to those obtained from commercially available software such as DigiSim or DigiElch. Excellent agreement was always achieved.

RESULTS AND DISCUSSION

The electrochemical behavior of the highly negatively charged anion of Rb_8K_2-**1**(0) is strongly influenced by pH and the identity of alkali metal cations present in the supporting electrolyte.[8] This is consistent with the importance of ion-pairing and involvement of protons or cations in the electron transfer steps. To further elucidate details associated with each electron transfer process and the role of the supporting electrolyte, electrochemical experiments in this study were performed in two acidic media (HCl or H_2SO_4), and the effect of the addition of KCl to HCl solutions (or 0.25 K_2SO_4 in the case of H_2SO_4) was also investigated.

Electrochemistry of the $\{Ru_4O_4(OH)_2(H_2O)_4\}$ Core. *Aqueous HCl Electrolyte.* Figure 1 shows dc cyclic voltammograms obtained over the potential range of −0.1 to 1.275 V vs Ag/AgCl (3 M NaCl) at a slow scan rate of 0.025 V s^{-1} when a glassy carbon electrode is in contact with 0.7 mM Rb_8K_2-**1**(0)

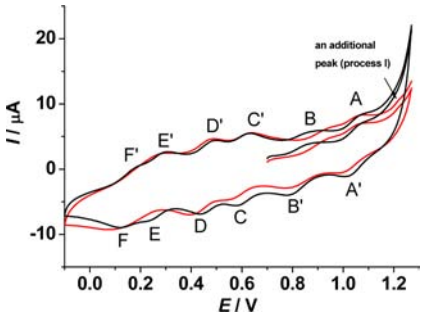

Figure 1. DC cyclic voltammograms obtained from a glassy carbon electrode in contact with 0.7 mM Rb_8K_2-**1**(0) in 0.1 M HCl in the presence (black solid line) and absence (red solid line) of 0.5 M KCl aqueous electrolyte solution. Experimental conditions: E_{start} = 0.70 V, E_{switch} = 1.275 and −0.10 V, E_{final} = 1.275 V, ν = 0.025 V s^{-1}. Reduction and oxidation components of six well resolved processes detected within the potential range shown are designated by letters A to F. Process I is just detectable prior to the solvent limit, in the absence of 0.5 M KCl in the electrolyte.

in 0.1 M HCl aqueous electrolyte solution in the presence and absence of 0.5 M KCl. The open circuit potential of 0.7 V vs Ag/AgCl (consistent with the zero current potential from RDE voltammogram, vide infra) was chosen as the initial potential to ensure that there is no redox chemistry occurring prior to scanning the potential. Use of this protocol is extremely important for the correct assignment of Rb_8K_2-**1**(0) redox processes with respect to whether they are associated with oxidation or reduction. Scanning of potential was commenced in the positive potential direction. Over the potential range mentioned above, there are a total of six processes, designated by symbols A′/A to F/F′. On the basis of peak-to-peak separations (ΔE_p values) which increase as the level of reversibility diminishes, the apparent electron transfer processes are slower in HCl solution without KCl (see Table 1). However, processes E/E′ and F/F′ are not resolved. Intriguingly, in the absence of 0.5 M KCl, an additional process is evident at ∼1.21 V (process I, Figure 1). Presumably, this oxidation process occurs at a more positive potential when KCl is present in the electrolyte, and therefore can occur prior to or beyond the solvent limit, depending on the electrolyte. This process will be considered in more detail below.

ΔE_p values provide an indication of the number of electrons transferred in a process if the electron transfer steps and coupled chemical reactions are all reversible. The ΔE_p values at a very slow scan rate of 0.025 V s^{-1} for processes A′/A to F/F′ (except for B′/B) suggest that they involve reversible one electron transfer steps, while the significantly larger ΔE_p for process B′/B is consistent with slow electron transfer (quasi-reversible behavior). At the initial potential of 0.7 V (open circuit potential), the Ru centers in the Rb_8K_2-**1**(0) system, both near to the electrode surface and in the bulk solution, will exist in the Ru_4(IV,IV,IV,IV) redox state. Consequently, processes A′/A and B′/B observed in the more positive potential region are each assigned to the one-electron oxidation of a Ru(IV) center to form a Ru(V) one. That is, they are $Ru^{IV/V}$ processes. In contrast, each of the four processes C/C′ to F/F′ observed in the more negative potential region are each assigned to the one-electron reduction of Ru(IV) center to form Ru(III), that is, they are $Ru^{IV/III}$ processes.[7,8,28] Rb_8K_2-**1**(0) has four Ru^{IV} centers,[7−9] which in principle can all be reduced and oxidized by one-electron. Earlier, we performed the redox titration of Rb_8K_2-**1**(0). The spectra of five stable complexes with different oxidation states of Ru4-core are reported.[8] The complex with Ru_4(IV,IV,IV,V) redox state has been isolated and comprehensively characterized.[8] On this basis, two additional $Ru^{IV/V}$ processes also should be available, lying at more positive potentials than the solvent limit of slightly greater than 1.20 V at a glassy carbon electrode. One of these appears to be just observable at ∼1.21 V in 0.1 M HCl in the absence of 0.5 M KCl.

The peak currents for all processes scale approximately with square root of scan rate over the range of 0.025 to 0.250 V s^{-1}, indicating diffusion control. However, the background current increases more rapidly (linearly) with scan rate, making detailed analysis of voltammograms at high scan rates problematical. On the basis of the ΔE_p dependence on scan rate, the ruthenium redox processes B′/B, E/E′, and F/F′ (quasi-reversible) exhibit an apparently slower rate of electron transfer than A′/A, C/C′, and D/D′ (reversible). As a consequence of the peak potential dependence on scan rate, the quasi-reversible, processes A′/A and B′/B, E/E′ and F/F′ merge at higher scan rates.

Figure 2 contains FT ac voltammograms obtained at a glassy carbon electrode for 0.7 mM Rb_8K_2-**1**(0) in 0.1 M HCl in the presence and absence of 0.5 M KCl. The same potential scanning protocol was employed as in dc cyclic voltammetry, but data for the initial 0.70 to 1.25 V region are omitted for clarity of presentation in this and other ac voltammograms. When 0.5 M KCl is present, the fundamental (first) to eighth harmonic components are shown. In the absence of 0.5 M KCl, only the third to sixth harmonics are shown. The fundamental harmonic component, as in dc cyclic voltammograms, includes a large background current contribution. In contrast, the second harmonic contains only a minimal level of background

Table 1. Comparison of DC Cyclic Voltammetric Data Obtained at a Glassy Carbon Electrode for 0.7 mM Rb_8K_2-1(0) at 0.025 V s^{-1} in 0.1 M HCl and 0.05 M H_2SO_4 Media in the Presence or Absence of 0.5 M K^+

medium	process	A/A′	B/B′	C/C′	D/D′	E/E′	F/F′
0.1 M HCl + 0.5 M KCl	$E^{\circ\prime}$ [a] (mV)	1039	842	602	465	272	153
	ΔE_p [b] (mV)	64	127	60	62	64	64
0.1 M HCl	$E^{\circ\prime}$ (mV)	1028	860	596	440	285 [c]	75 [d]
	ΔE_p (mV)	85	161	90	93		
0.05 M H_2SO_4 + 0.25 M K_2SO_4	$E^{\circ\prime}$ (mV)	991	760	541	417	203	106
	ΔE_p (mV)	77	68	58	58	60	60
0.05 M H_2SO_4	$E^{\circ\prime}$ (mV)	1004	797	563	424	235 [c]	102 [d]
	ΔE_p (mV)	79	96	67	64		

[a]Reversible potentials, $E^{\circ\prime}$, derived from the average of the oxidation and reduction peak potentials = $(E_p^{ox} + E_p^{red})/2$. [b]Peak-to-peak separation, $\Delta E_p = E_p^{ox} - E_p^{red}$. [c]$E_p^{ox}$ only, E_p^{red} difficult to detect. [d]E_p^{red} only, E_p^{ox} difficult to detect.

dx.doi.org/10.1021/ic301370y | Inorg. Chem. 2012, 51, 11521−11532

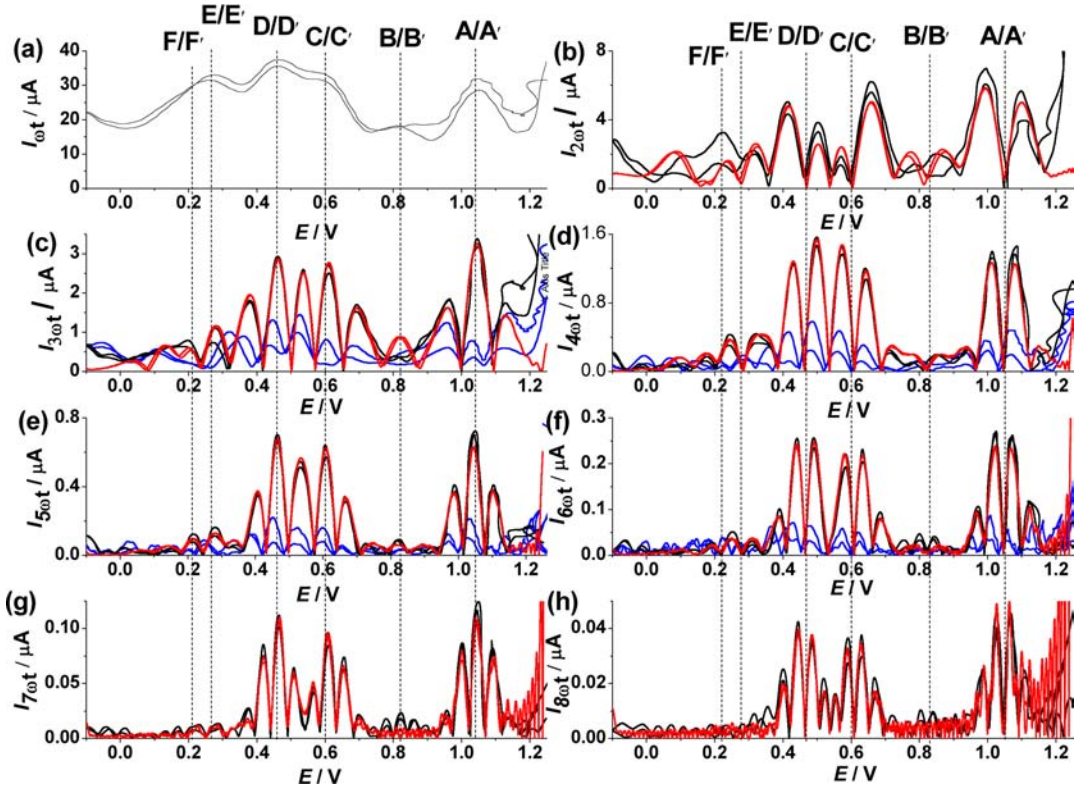

Figure 2. FT ac cyclic voltammetric fundamental (a) to eighth (h) harmonic components for $Ru^{IV/V}$ oxidation (A/A′, B/B′) and $Ru^{IV/III}$ reduction (C/C′, D/D′, E/E′, F/F′) obtained at a glassy carbon electrode for 0.7 mM Rb_8K_2-**1**(0) in 0.1 M HCl aqueous electrolyte solution in the presence (black solid line) and absence (blue solid line, only the third to sixth harmonics are shown in this case) of 0.5 M KCl. E_{start} = 0.70 V, E_{switch} = 1.25 and −0.10 V, E_{final} = 1.25 V, f = 9.02 Hz, ΔE = 0.08 V, v = 0.0605 V s^{-1}. Reversible potentials associated with each process are designated by a reference line estimated from dc cyclic voltammograms. Simulation (red solid line) parameters for second (b) to eighth (h) ac harmonics are as experimental parameters, with $E^{o\prime}_{A/A'}$ = 1.045 V, $E^{o\prime}_{B/B'}$ = 0.820 V, $E^{o\prime}_{C/C'}$ = 0.608 V, $E^{o\prime}_{D/D'}$ = 0.465 V, $E^{o\prime}_{E/E'}$ = 0.280 V, $E^{o\prime}_{F/F'}$ = 0.140 V, $k^{o\prime}_{A/A'}$ = 0.027 cm s^{-1}, $k^{o\prime}_{B/B'}$ = 0.003 cm s^{-1}, $k^{o\prime}_{C/C'}$ = 0.022 cm s^{-1}, $k^{o\prime}_{D/D'}$ = 0.027 cm s^{-1}, $k^{o\prime}_{E/E'}$ = 0.005 cm s^{-1}, $k^{o\prime}_{F/F'}$ = 0.0025 cm s^{-1}, R_u = 80 Ω, C_{dl} = 60 μF cm^{-2}, α = 0.5, D = 1.80 × 10^{-6} cm^2 s^{-1}. For all processes, n = 1.

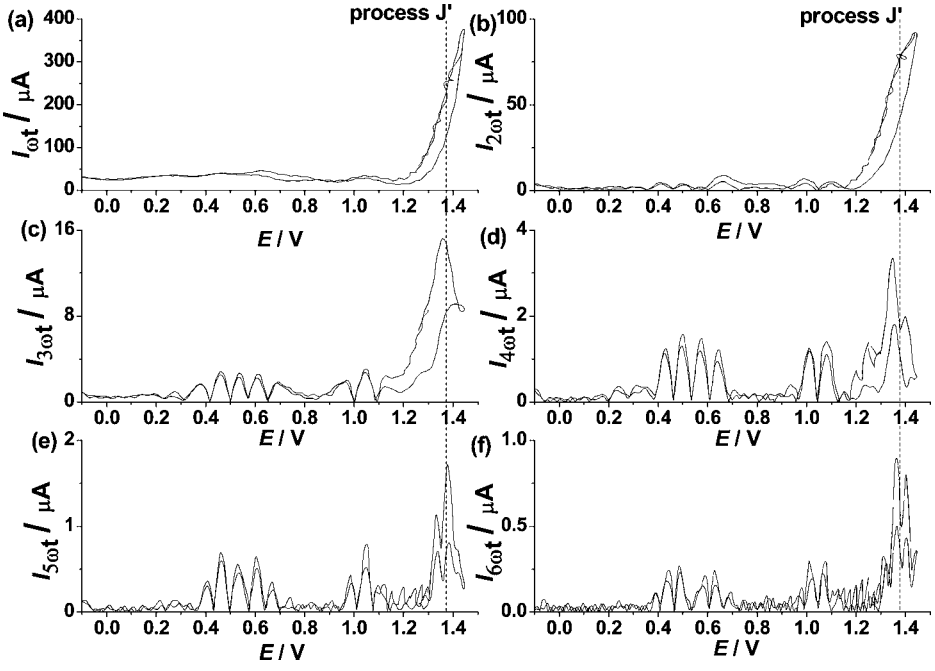

Figure 3. FT ac cyclic fundamental (a) to sixth (f) harmonic voltammetric components obtained at glassy carbon electrode for 0.7 mM Rb_8K_2-**1**(0) in 0.5 M KCl + 0.1 M HCl aqueous electrolyte solution. E_{start} = 0.70 V, E_{switch} = 1.45 and −0.10 V, f = 9.0 Hz, ΔE = 0.08 V, v = 0.0605 V s^{-1}. Process J is now seen under these conditions.

dx.doi.org/10.1021/ic301370y | *Inorg. Chem.* 2012, 51, 11521−11532

current, and exhibits a much improved faradaic to background current ratio. Purely faradaic signals that are devoid of background current are obtained in the fourth and higher harmonic components. In ac voltammetry, the peak current magnitude directly reflects the kinetics of the electron transfer process. Comparatively, in the presence of 0.5 M KCl, the $Ru^{IV/V}$ (A′/A) and $Ru^{IV/III}$ processes (C/C′ and D/D′) provide a significantly larger current which implies a much faster electron transfer rate compared to processes B′/B, E/E′, and F/F′. Comparison with a simulated voltammogram (with the assumption of fully reversible proton coupled electron transfer) indicates an order of magnitude increase in the apparent rate constants ($k^{o\prime}$) of processes A′/A, C/C′, and D/D′ ($k^{o\prime}_{A/A'}$ = 0.027 cm s^{-1}, $k^{o\prime}_{C/C'}$ = 0.022 cm s^{-1}, $k^{o\prime}_{D/D'}$ = 0.027 cm s^{-1}) than those of processes B′/B, E/E′, and F/F′ ($k^{o\prime}_{B/B'}$ = 0.003 cm s^{-1}, $k^{o\prime}_{E/E'}$ = 0.005 cm s^{-1}, $k^{o\prime}_{F/F'}$ = 0.0025 cm s^{-1}). In the simulations, the charge transfer coefficient, α, was always assumed to be 0.5, the diffusion coefficient of all species (1.80 ± 0.04) × 10^{-6} cm^2 s^{-1} (see below), and $E^{o\prime}$ was taken to be the value derived from the dc cyclic midpoint potentials. The significantly smaller ac peak current magnitude detected in the Rb_8K_2-**1**(0) system in the absence of 0.5 M KCl reflects the apparently slower electron transfer rate and implies the addition of K^+ enhances the rate.[20] Analysis of ac data in the context of apparent electron transfer rates is in excellent agreement with the conclusions derived from dc cyclic voltammograms (Figure 1). In the absence of KCl, simulations based on a simple electron transfer model are complicated by overlapping of processes and hence were not attempted.[29] However, slower electron transfer is assumed to apply as judged from both ΔE_p values in dc voltammograms and peak current magnitudes in ac voltammograms. The $k^{o\prime}$ values are regarded as apparent because $E^{o\prime}$ values include terms for protonation and/or ion pairing with K^+. Note that in the sixth harmonic, process I′/I is just detectable near 1.20 V, but the low current magnitude and consequently poor signal-to-background noise ratio prohibits quantitative analysis of this process.

In principle, and as noted above, additional processes involving $Ru^{IV/V}$ oxidation are predicted to occur at a very positive potential. The ac method allows more positive potentials to be probed because the method is very insensitive to the highly irreversible water oxidation process. Figure 3 provides ac fundamental to sixth harmonic voltammograms when the potential range is extended from 1.25 to 1.45 V. In the fundamental (Figure 3a) and second harmonic components (Figure 3b), substantial current from solvent oxidation is still detected at potentials slightly more positive than 1.2 V. However, in the fourth and higher harmonic components, the solvent limit is found at more positive potentials and well-defined $Ru^{IV/V}$ faradaic electrochemistry is detected (process J′/J, $E^{o\prime}$ ∼ 1.40 V). Thus, the ac method allows detection of an additional fourth $Ru^{IV/V}$ process. This process will be even more clearly seen in ac voltammetry in sulfuric acid electrolyte (see later).

In the study reported by Bonchio and co-workers, processes C/C′, B/B′, and A′/A, were all assigned to one-electron oxidation $Ru^{IV/V}$ processes.[10] This contradicts our findings where process C/C′ is deduced to be a reduction step. Cyclic voltammetry is not an ideal method for assigning the redox processes given the complexity of the redox chemistry of Rb_8K_2-**1**(0) and the fact that as many as 6 processes in total are observed in a potential range of less than 1 V. To confirm that the assignment of the processes based on our interpretation of cyclic voltammetric data are correct, the steady-state rotating disk electrode (RDE) method was employed. The advantage of the steady-state voltammetric techniques, such as RDE voltammetry, is that the voltammetric response is independent of the initial potential.[30] Therefore, regardless of the starting potential, any process producing positive steady-state diffusion-controlled limiting current is an oxidation process, whereas any process producing negative steady-state diffusion-controlled limiting current is a reduction one. Figure 4a shows the RDE

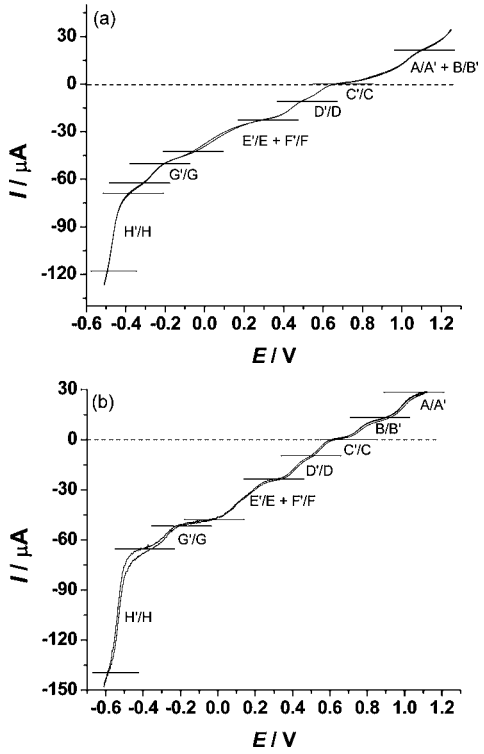

Figure 4. Glassy carbon rotating disk electrode voltammogram (step regions marked) for 0.7 mM Rb_8K_2-**1**(0) in (a) 0.5 M KCl + 0.1 M HCl, and (b) 0.25 M K_2SO_4 + 0.05 M H_2SO_4, ω = 105 rad s^{-1}, ν = 0.01 V s^{-1}.

voltammogram obtained at a rotation rate of 104.7 rad s^{-1} with a glassy carbon electrode for 0.7 mM Rb_8K_2-**1**(0) in 0.1 M HCl in the presence of 0.5 M KCl aqueous electrolyte. While slow scan rate cyclic voltammograms in this medium display six resolved processes designated A′/A to F/F′ (Figure 1), at the rotating disk electrode, processes with slower electron transfer (B′/B, E/E′, and F/F′) now overlap with neighboring processes, so that processes A′/A+B′/B and E/E′+F/F′ now appear as apparently two electron processes. Processes E/E′+F/F′ were highly sensitive to the condition of the electrode surface, appearing as resolved single electron transfer process (at low scan rate) with a well polished working electrode. Importantly, the zero current at the potential of +0.7 V (vs Ag/AgCl) shows convincingly that processes A′/A and B′/B are oxidation steps as evidenced by their positive steady-state diffusion-controlled limiting currents, and all others are reduction processes that exhibit negative current. The plots of I_L vs $\omega^{1/2}$ for the reversible processes were linear for the rotation rate (ω) range of 52−314 rad s^{-1}, indicating that mass transport-controlled reactions occur in the limiting current region. Plots of E vs $\ln[(I_L - I)/I]$ were linear at a rotation rate of 52.4 rad s^{-1} and estimates of n = 1.0 (±0.2) were obtained

dx.doi.org/10.1021/ic301370y | Inorg. Chem. 2012, 51, 11521−11532

from the slope (RT/nF) for process C/C′. The diffusion coefficient of Rb_8K_2-**1**(0) is calculated to be $(1.80 \pm 0.05) \times 10^{-6}$ cm^2 s^{-1} using the Levich equation.[30] The RDE voltammetric data are fully consistent with the results obtained from ac and dc cyclic voltammetry.

Aqueous H_2SO_4 Electrolyte. Similar to the results obtained in HCl medium, under dc conditions the tetraruthenium centers exhibit two oxidation and four reduction processes with 0.05 M H_2SO_4 (pH 1.45, ionic strength 0.08 M) also containing 0.25 M K_2SO_4 (pH 2.0, ionic strength 0.73 M) as the electrolyte. The oxidation processes are again assigned to the oxidation of two Ru(IV) centers to Ru(V) ($Ru^{IV/V}$ redox chemistry),[7,8,28] and no further oxidation was observed in the potential range available (up to +1.3 V vs Ag/AgCl, the solvent limit). The reduction processes are assigned to conversion of all four Ru(IV) centers to the Ru(III) redox state. The peak current magnitudes of all processes are proportional to the square root of the scan rate, indicating diffusion control at their peak potentials. The peak current values are similar to those obtained in 0.1 M HCl medium containing 0.5 M KCl. However, ΔE_p values for a given scan rate are smaller (except for process A′/A) (Table 1), indicating apparently faster electron transfer kinetics in sulfate containing electrolyte. The two reduction processes with reversible potentials of about +0.203 V (process E/E′) and +0.106 V (process F/F′) are well-resolved under the conditions of Figure 5 at all scan rates

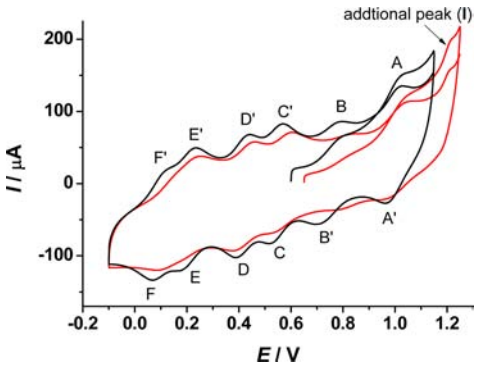

Figure 5. DC cyclic voltammograms obtained from a glassy carbon electrode in contact with 0.7 mM Rb_8K_2-**1**(0) in 0.05 M H_2SO_4 in the presence (black solid line) and absence (red solid line) of 0.25 M K_2SO_4 aqueous electrolyte solution. ν = 3.0 V s^{-1}.

studied (0.025 V s^{-1} to 3.0 V s^{-1}), which implies that the kinetics are reasonably fast, in contrast to the results obtained in 0.1 M HCl in the presence of 0.5 M KCl, where these two reduction processes merged as the scan rate was increased. This kinetic difference might be due to the differences in pH and ionic strength in these systems. While, both acids nominally have an equal molarity of H^+ derived from 0.05 M H_2SO_4 vs 0.10 M HCl, the pH value measured in the sulfuric acid (diprotic acid) medium, which also contains HSO_4^-, is 1.45, which is about 0.2 units higher than that measured in the HCl (monoprotic acid) medium in the absence of K^+ salt. In the presence of K^+ salt, the mixture of 0.05 M H_2SO_4 + 0.25 M K_2SO_4 is a sulfate buffer with measured pH 2.0, which is 0.8 units higher than that measured in 0.1 M HCl + 0.5 M KCl (pH 1.2). The presence of K^+ salt also significantly increases the ionic strength.

RDE voltammograms in aqueous sulfuric acid in the presence of 0.25 M K_2SO_4 exhibited two well-resolved oxidation processes and four reduction processes when using rotation rates in the range of 52−314 rad s^{-1}. Plots of I_L vs $\omega^{1/2}$ for all six processes indicated that the estimation of n = 1.0 (±0.2) is applicable for all processes. The RDE voltammograms (Figure 4b) also exhibit well resolved processes E/E′ and F/F′ under these conditions.

In the absence of the K^+ cation, the rest potential occurred at a more positive value, which is consistent with data at lower pH. An additional oxidation process could just be observed at about +1.2 V, which again mimics behavior obtained in 0.1 M HCl when K^+ is absent. This oxidation process is again assigned to the oxidation of Ru^{IV} to Ru^V of a third Ru^{IV} center. Processes A′/A and D/D′ shifted slightly more positive (13 mV for A′/A and 7 mV for D/D′), but process C/C′ shifted about 27 mV more positive in the absence of K^+. However, the absence of K^+ affected processes E/E′ and F/F′ more severely. They now become merged (process F/F′ shifted to more positive potential, closer to process E/E′) and could not be resolved at all scan rates studied (Figure 5). The RDE voltammograms also show the merging of these two processes (not shown). The peak-to-peak separations (ΔE_p) for all these redox processes are larger in the absence of K^+. This again is consistent with the conclusion that the apparent electron transfer kinetics of these ruthenium centered redox are slower in the absence of K^+. Figure 6 shows the ac voltammograms obtained at a glassy carbon electrode for 0.7 mM Rb_8K_2-**1**(0) in 0.05 M H_2SO_4 in the presence (fundamental to eighth harmonics) and absence of 0.25 M K_2SO_4 (third to sixth harmonics). In the presence of 0.5 M K^+, the fundamental harmonic shows a much higher background current than that obtained in 0.1 M HCl, and the magnitude of the faradaic current is also higher. In the second harmonic, where the background current is relatively small compared to the faradaic current, the peak currents obtained in 0.05 M H_2SO_4 are nearly twice those obtained in 0.1 M HCl, which again implies that the apparent electron transfer kinetics of the ruthenium centered redox processes are much faster in 0.05 M H_2SO_4 than in 0.1 M HCl (noting again that the peak current magnitude directly reflects the kinetics of the electron transfer process in ac voltammetry). The higher harmonic data, where faradaic signals are devoid of background current, are consistent with the second harmonic data.

It is also apparent from the ac data that the apparent electron transfer kinetics of redox processes E/E′ and F/F′ are much faster in 0.05 M H_2SO_4 than in 0.1 M HCl, as evidenced by their peak currents now being similar to those of redox processes C/C′ and D/D′. Simulated ac harmonic data agrees well with this observation where the apparent rates of electron transfers are $k^{o\prime}_{B/B'}$ = 0.010 cm s^{-1}, $k^{o\prime}_{E/E'}$ = 0.030 cm s^{-1}, $k^{o\prime}_{F/F'}$ = 0.015 cm s^{-1}) while processes A′/A, C/C′, and D/D′ appear to be fully reversible ($k^{\circ\prime}$ > 1 cm s^{-1}). The conclusions derived from ac data again agree well with the dc data. In the 0.1 M HCl electrolyte case, adsorption of Cl^- on the electrode surface could hinder the electron transfer rate.[32] Complexation of the Cl^- anion with the Ru4-core[8,31] is less likely to affect the rate.

Ac voltammetric Investigations encompassing an extended range of potential (switching potential of 1.45 V), as is the case in 0.1 M HCl containing 0.5 M KCl, allowed a fourth oxidation process (process J′/J) to be readily detected at very positive potentials (∼ 1.32 V), which is well beyond the dc solvent oxidation limit, and hence could not be detected under dc conditions. This process is assigned to the oxidation of the fourth Ru^{IV} center. The third $Ru^{IV/V}$ process (I) is undetectable

dx.doi.org/10.1021/ic301370y | *Inorg. Chem.* 2012, 51, 11521−11532

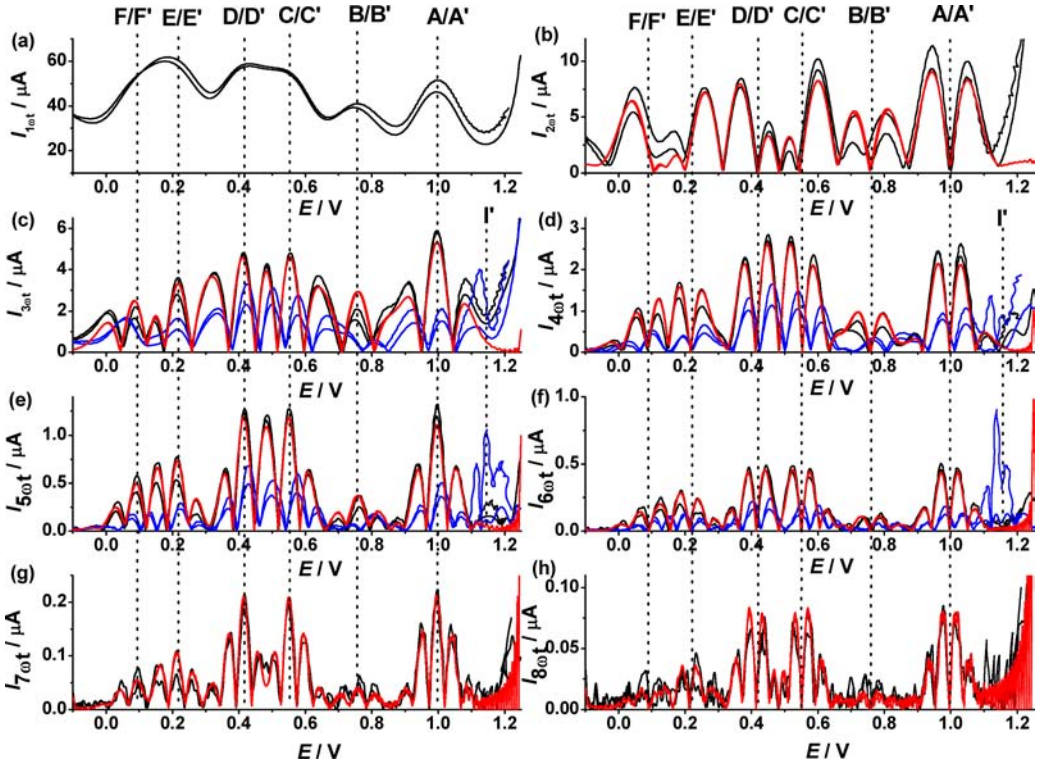

Figure 6. FT ac cyclic fundamental (a) to eighth (h) harmonic voltammetric components for $Ru^{IV/V}$ oxidation (A/A′, B/B′) and $Ru^{IV/III}$ reduction (C/C′, D/D′, E/E′, F/F′) obtained at a glassy carbon electrode for 0.7 mM Rb_8K_2-**1**(0) in 0.05 M H_2SO_4 aqueous electrolyte solution in the presence (black solid line) and absence (blue solid line, only third to sixth harmonics are shown in this case) of 0.25 M K_2SO_4 aqueous electrolyte solution. E_{start} = 0.70 V, E_{switch} = 1.25 V = −0.10 V, E_{final} = 1.25 V, f = 9.02 Hz, ΔE = 0.08 V, v = 0.0615 V s^{-1}. Reversible potentials associated with each process are designated by a reference line estimated from dc cyclic voltammogram. Simulation (red solid line) parameters for second (b) to eighth (h) ac harmonics are as experimental parameters, with $E^{o\prime}_{A/A'}$= 0.996 V, $E^{o\prime}_{B/B'}$= 0.758 V, $E^{o\prime}_{C/C'}$= 0.551 V, $E^{o\prime}_{D/D'}$= 0.414 V, $E^{o\prime}_{E/E'}$= 0.214 V, $E^{o\prime}_{F/F'}$= 0.0923 V, $k^{o\prime}_{A/A'}$= 1.0 cm s^{-1}, $k^{o\prime}_{B/B'}$= 0.012 cm s^{-1}, $k^{o\prime}_{C/C'}$= 1.0 cm s^{-1}, $k^{o\prime}_{D/D'}$= 1.0 cm s^{-1}, $k^{o\prime}_{E/E'}$= 0.03 cm s^{-1}, $k^{o\prime}_{F/F'}$= 0.015 cm s^{-1}, R_u= 80 Ω, C_{dl} = 60 μF cm^{-2}, α = 0.5, D = 1.80 × 10^{-6} cm^2 s^{-1}. For all processes n = 1.

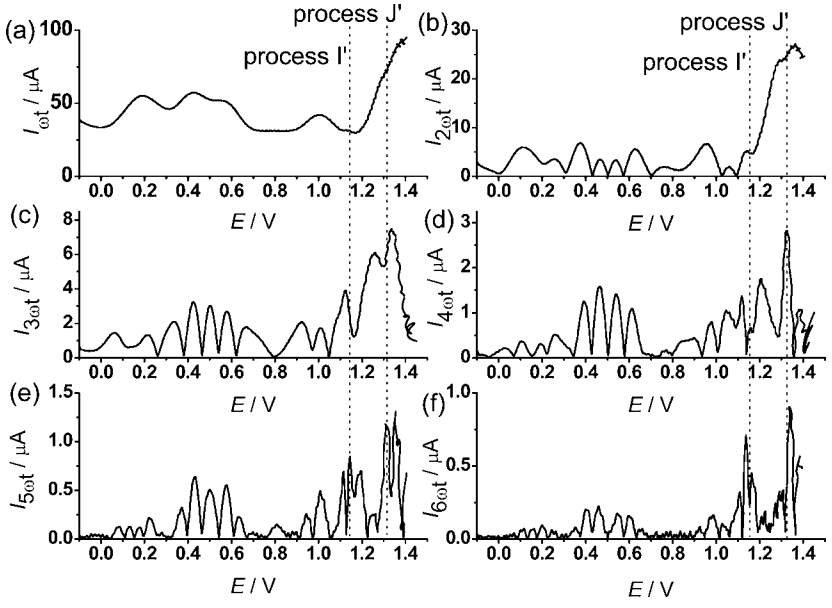

Figure 7. FT ac cyclic fundamental (a) to sixth (f) harmonic voltammetric components for the Ru_4-core obtained at glassy carbon electrode for 0.7 mM Rb_8K_2-**1**(0) in 0.05 M H_2SO_4 aqueous electrolyte solution. E_{start} = −0.10 V, E_{switch} = −0.60 V, f = 9.0 Hz, ΔE = 0.08 V, v = 0.0605 V s^{-1}.

in the higher harmonic components, presumably because of a slow electron transfer rate.

In the absence of added K^+, the electron transfer kinetics of processes A′/A, C/C′, and D/D′ decreased relative to those in the presence of K^+, as evidenced by their diminished peak current magnitudes. The third and higher harmonics of redox processes B′/B, E/E′, and F/F′ are now not as well-defined, and have very small peak currents, indicating slow electron

dx.doi.org/10.1021/ic301370y | Inorg. Chem. 2012, 51, 11521−11532

transfer. These results agree well with the dc data. However, in the fifth and sixth harmonics, the process at ~1.15 V matched that of process I′/I identified from the dc cyclic voltammogram (see Figure 5). AC voltammetric experiments with extended positive potential limit (1.45 V), now exhibit two well-defined processes (Figure 7, only oxidative scan is shown) in the fifth and sixth harmonics at potentials of ~1.15 V and ~1.32 V, respectively. These processes are assigned to the third and fourth $Ru^{IV/V}$ oxidation steps (process I′/I and J′/J). This result again shows the distinct advantage of employing analysis based on higher harmonic components derived from large-amplitude ac voltammetry, with respect to the resolution of processes overlapping with the underlying solvent limit reaction.

On the basis of data combined from both dc and ac methods, plots for the reversible potentials for the oxidation ($Ru^{IV/V}$) and reduction ($Ru^{IV/III}$) processes of each four centers in both 0.1 M HCl and 0.05 M H_2SO_4 media in the presence and in the absence of KCl/K_2SO_4 are shown in Figure 8. All data appeared

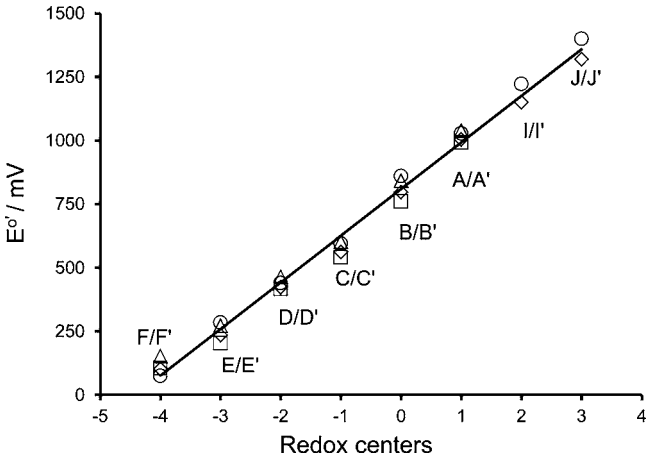

Figure 8. Plots of apparent reversible potential $E^{\circ\prime}$ for the redox levels of the four oxidation and four reduction processes of the four Ru centers in 0.1 M HCl (○), 0.05 M H_2SO_4 (◇), 0.1 M HCl + 0.5 M KCl (△), and 0.05 M H_2SO_4 + 0.25 M K_2SO_4 (□). Processes are indicated by letters A to F, and I and J as described in the text. The $E^{\circ\prime}$ values are determined based on experimental conditions as in Figures 2, 3, and 6 and Table 1.

to lie on the same straight line with a slope of about 185 mV per change in oxidation state of Ru_4-core. This outcome is an extension of data published for the first two oxidation and four reduction processes.[7,8,28] Previously, only two oxidation processes of $Ru^{IV/V}$ were identified. However, in this study, dc or ac methods with a suitably acidic medium, allow the third $Ru^{IV/V}$ process to be identified, and the ac method reveals the underlying fourth $Ru^{IV/V}$ process which lies at potentials well beyond the dc solvent limit. The data in Figure 8 can be also used to help identify the reactive species which oxidize water under acidic conditions via a four-electron process. Four electron reduction of $\mathbf{1}(3)$ could produce $\mathbf{1}(-1)$ and O_2. In acidic media, the average potential for this transformation is ~1.1 V (NHE), which is lower than required by thermodynamics, ~1.2 V. However, the average potential for the $\mathbf{1}(4) \rightarrow \mathbf{1}(0)$ transformation, ~1.3 V, is sufficient to oxidize water. Also it is noted that the Ce(IV) /Ce(III) couple, 1.72 V, used to create a catalytic cycle in acid media,[9] is higher than that of the $\mathbf{1}(4)/\mathbf{1}(3)$ couple, ~1.55 V. On these grounds, $\mathbf{1}(4)$ is the most likely candidate for the O_2 releasing species in acid media.

Electron Transfer Reactions in the Presence of Potassium Cations. A significant increase of the rate of homogeneous POM electron transfer reactions on addition of K^+ has been described in the literature.[20,31] This acceleration cannot be solely attributed to an increase in the ionic strength and strongly depends on the nature of the cation. In this scenario, partial dehydration of K^+ results in formation of a contact ion pair in which the electron transfer is facilitated through a bridging potassium cation. The Gibbs free energy of hydration of M^+ is less negative in the sequence $H^+ \ll Na^+ < K^+$,[32] which is consistent with a larger effect of the potassium cation. Such a mechanism, which also should be relevant to heterogeneous electron transfer that occurs at the electrode surface, requires formation of a solvent separated ion-pair of a cation and a POM, which after dehydration becomes a contact ion pair. The ion pair formation constants estimated from Fuoss equation[33] decrease with ionic strength. Conventional ion pairing is not extensive enough to explain the enhanced electron transfer kinetics at high potassium concentration.[20]

In the case of a solvent separated ion-pair with the POM of interest in this study and assuming the theory is valid at high ionic strength, then the number of cations, m, with a hydrodynamic radius r_h, located on the POM surface can be estimated from eq 1

$$m \approx (4\pi R^2)(2r_h)N_A[M^+] \quad (1)$$

where R is the radius of POM, N_A is Avogadro's number, and $[M^+]$ is the concentration of a cation M^+.[34] $\mathbf{1}(n)$ is now used to designate the Ru_4-core located between two (γ-$SiW_{10}O_{36}$) spheres with R = 5.5 Å, but only half of these spherical surfaces is accessible by K^+ cations of hydrodynamic radius in the range of 1.22−3.31 Å,[20] then m ~ 0.3−0.8 for each (γ-$SiW_{10}O_{36}$) or m ~ 0.6−1.6 per Ru_4POM with 0.5 M KCl as electrolyte is yielded. This implies that at high electrolyte concentrations $\mathbf{1}(n)$ is mostly present as a solvent separated ion pair with one potassium cation (henceforth $\mathbf{1}\|K^+$). Partial dehydration of the cation will form a *contact* ion pair (henceforth $\mathbf{1}K^+$).

Under conditions where the hydronium cation concentration is much lower than $[K^+]$ and where the dehydration is thermodynamically much less favorable, ion-pairing with H^+ can be ignored. In earlier work, we have shown[7,8] that $\mathbf{1}(0)$ is a weak diprotic acid with two pK_a values around 4. When the pH is increased from 2 to 5, significant changes in UV−vis spectra occur indicating that the Ru_4-core is involved in acid−base equilibria. On this basis, the solvent separated ion pair of protonated $\mathbf{1}(n)$ (henceforth $\mathbf{1}H^+$) with K^+ should be also considered: $\mathbf{1}H^+\|K^+$, so that one electron reduction of $\mathbf{1}(n)$ results in formation of species such as: $\mathbf{1}^-K^+$, $\mathbf{1}^-\|K^+$, and $\mathbf{1}^-H^+\|K^+$. Consequently, Scheme 1 can be proposed for the 1-electron reduction of $\mathbf{1}(n)$ in the presence of a high concentration of K^+:

In accordance with this Scheme, contact ion pairs $\mathbf{1}K^+$ and $\mathbf{1}^-K^+$ are the dominant electrochemically active species in the presence of a high concentration of K^+, and their concentrations are pH dependent. Analogous types of reaction schemes would apply to the proton. Consequently, the effect of pH on the redox properties of $\mathbf{1}(n)$ in the presence of K^+ was studied.

pH Effect on Redox Properties of Ru-Centers. Figure 9 shows the pH-dependence of four processes, two respectively from the oxidation of $Ru^{IV/V}$ (processes B′/B and A′/A) and two from reduction of $Ru^{IV/III}$ (processes C/C′ and D/D′) in the presence of 0.5 M KCl. These four processes are readily

Scheme 1. Reaction Pathways for the 1-Electron Reduction of 1(n) in the Presence of a High Concentration of Potassium Cations

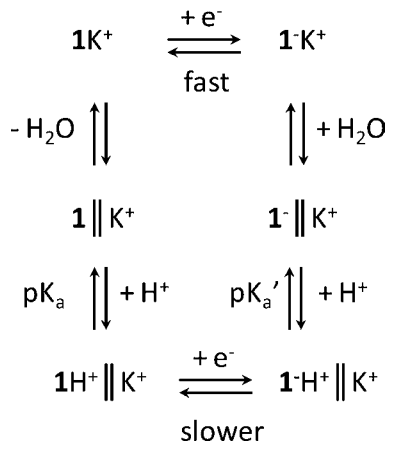

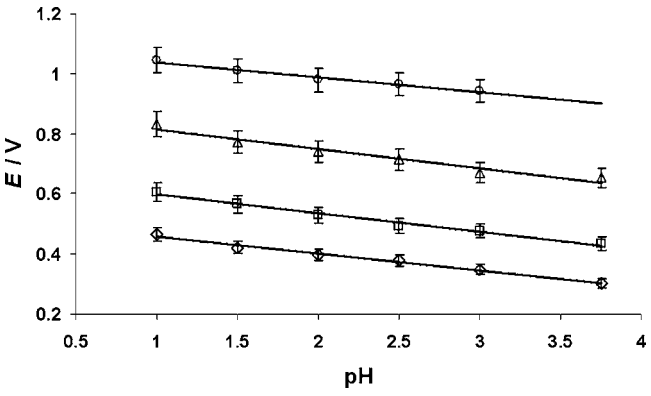

Figure 9. Reversible potentials of redox processes A′(○), B′ (△), C′ (□), and D′ (◇) as a function of pH. The experimental conditions used to obtain the data are described in the text.

identified under conditions of dc cyclic voltammetry at pH values of 3.80 and lower. The measurements of reversible potentials were initially performed on Rb_8K_2-1(0) solutions containing 0.5 M KCl with a pH of 3.80. Then, HCl or NaOH was added to alter the pH. With increasing acidity, the potentials for all processes B′/B, A′/A, C/C′, and D/D′ shifted to more positive values. It is noteworthy that the processes E/E′ and F/F′ also become better defined, but they are too close to accurately measure the pH dependence of their redox potentials. The slopes of a plot of reversible potential versus pH for the first two oxidation and first two reduction processes were 57 ± 6 mV, which is commonly interpreted as a one electron transfer reaction coupled with a proton transfer (the PCET mechanism in eq 2).[18,19,35,36] The question therefore arises as to whether the data in Figure 8 prove that oxidation/reduction of the Ru_4-core proceeds via the PCET (proton coupled electron transfer) mechanism in eq 2.

$$\mathbf{1}(n)\mathrm{H}^+ + \mathrm{e}^- = \mathbf{1}(n-1) + \mathrm{H}^+ \qquad (2)$$

Unfortunately the available data do not give an unambiguous answer. Specifically, one should not assume that this pH dependence observed in the acidic media will also be applicable to neutral pH conditions where high catalytic activity of **1** in water oxidation is observed. The full interpretation of data in Figure 9 requires detailed knowledge of acid–base properties of **1**(0) (pK_a and pK_a') and ion pairing details of both redox levels relevant to the processes of K^+. Studies required to fully interpret the pH and $[K^+]$ dependence of the voltammetry are in progress.

Electrochemistry of the Decatungstosilicate Framework. *Aqueous HCl Electrolyte.* Figure 10 shows dc cyclic

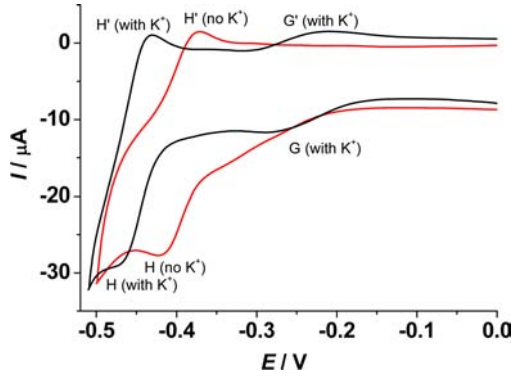

Figure 10. DC cyclic voltammograms for the polyoxometalate framework obtained at a glassy carbon electrode for 0.7 mM Rb_8K_2-**1**(0) in 0.1 M HCl in the presence (black solid line) and absence (red solid line) of 0.5 M KCl aqueous electrolyte solution. v = 0.025 V s^{-1}.

voltammograms at a scan rate of 0.025 V s^{-1} in the negative potential region for Rb_8K_2-**1**(0) in 0.1 M HCl aqueous electrolyte solution in the presence and absence of 0.5 M KCl. As for the Ru_4-centers, the addition of 0.5 M KCl produces apparently faster electron transfer as identified by the smaller ΔE_p values for process H/H′ of decatungstosilicate. Nevertheless, the effect of 0.5 M KCl on the polyoxometalate framework is not limited to kinetics, but also shifts the reversible potential of process H/H′ (no KCl, $E^{\circ\prime}$ = ∼ −400 mV; with KCl, $E^{\circ\prime}$ = ∼ −450 mV) to a more negative value indicating a higher level of protonation in the absence of KCl. Formation of a solvent separated ion-pair of highly reduced **1** with potassium cations is postulated to inhibit the protonation of tungstate network. Apart from that, process G/G′ now emerges because the H/H′ process shifts to more negative values in the presence of KCl.

As in the case of the ruthenium redox chemistry, limiting current analysis was derived from rotating disk electrode data (Figure 4a) for processes G/G′ and H/H′ with the rotation rates in the range of 52−314 rad s^{-1}. Plots of I_L vs $\omega^{1/2}$ for processes G/G′ and H/H′ were also linear, again indicating that mass transport-controlled reactions occur in the limiting current region. Estimates of n = 1.1 (±0.2) and 4.1 (±0.2) for processes G/G′ and H/H′, respectively, were obtained based on comparisons of the I_L values for processes G/G′ and H/H′ with those for the well resolved one-electron transfer processes C/C′ and D/D′. Thus, process G/G′, according to the current magnitude, seems to involve a one electron transfer.

Under conditions of cyclic voltammetry, the large size of Rb_8K_2-**1**(0) gives rise to a small diffusion coefficient, D, which means that the faradaic-to-background current ratios are not favorable; the I_p^{ox} and I_p^{red} values therefore have significant uncertainty. The multiple electron reduction of the tungstate framework in process H/H′ is very common in acidic medium, when electron and proton transfer are coupled.[16,17] The origin of process G/G′ will be discussed later.

AC cyclic voltammetric data (Figure 11) again provide access to faradaic processes devoid of background current. As in dc cyclic voltammograms, the peak current magnitude for process

dx.doi.org/10.1021/ic301370y | Inorg. Chem. 2012, 51, 11521−11532

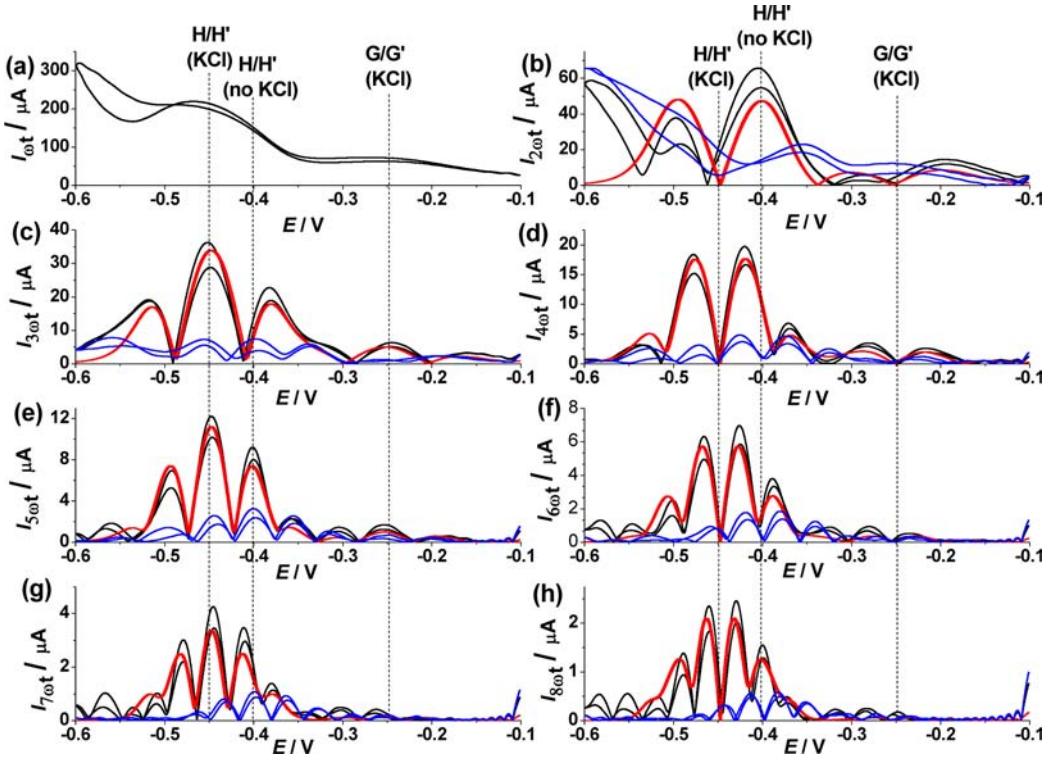

Figure 11. FT ac cyclic voltammetric fundamental (a) to eighth (h) harmonic components for the polyoxometalate framework obtained at a glassy carbon electrode for 0.7 mM Rb_8K_2-**1**(0) in 0.1 M HCl aqueous electrolyte solution in the presence (black solid line) and absence (blue solid line, only second to sixth harmonics are shown in this case) of 0.5 M KCl. E_{start} = −0.10 V, E_{switch} = −0.60 V, E_{final} = −0.10 V, f = 9.02 Hz, ΔE = 0.08 V, v = 0.08941 V s^{-1}. Reversible potentials associated with each process are designated by a reference line estimated from dc cyclic voltammogram. Simulation (red solid line) parameters for second (b) to eighth (h) ac harmonics are as experimental parameters, with $E^{o\prime}_{G/G'}$ = −0.253 V, $E^{o\prime}_{H/H'}(1)$ = −0.447 V, $E^{o\prime}_{H/H'}(2)$ = −0.447 V, $E^{o\prime}_{H/H'}(3)$ = −0.447 V, $E^{o\prime}_{H/H'}(4)$ = −0.447 V, all with $k^{o\prime}$ = 0.2 cm s^{-1}, R_u = 80 Ω, C_{dl} = 60 μF cm^{-2}, α = 0.5, D = 1.80 × 10^{-6} cm^2 s^{-1}. For all processes, n = 1, where process H/H′ is considered to consist of four sequential proton-coupled electron transfer steps (see text for details).

H/H′ in the presence of KCl under ac conditions is far larger than in the absence of KCl. Additionally, differences in the reversible potentials are also readily identified. The significantly larger current for the polyoxometalate process H/H′ is consistent with multiple electron transfer and a very fast reaction rate for each electron transfer step as is the case in the presence of KCl. The small peak current magnitude for process G/G′ (in the absence of 0.5 M KCl) makes this process difficult to identify under the ac conditions employed. To identify the origin of process G/G′, we used thin-layer spectroelectrochemistry to check whether a characteristic reduced polyoxometalate blue color is formed at potentials slightly more negative than G/G′. No significant spectral changes were observed. If the applied potential was more negative than H/H′, an intermediate formation of blue color was seen. This species with reduced W atom(s) is unstable and forms a dark film on the electrode surface. Therefore, the G/G′ process is likely to be a Ru^{III}/Ru^{II} reduction. For convenience, we discussed this process in this polyoxometalate framework section.

Simulations based on a simultaneous four-electron transfer reaction resulted in ac harmonic voltammograms with very much larger peak currents than found experimentally for process H/H′. Therefore, to mimic the voltammetry, the four electron transfer steps associated with process H/H′ are presumed to occur sequentially with proton-coupling rather than simultaneously. A one electron transfer ($E^{o\prime}$ = −0.25 V, $k^{o\prime}$ = 0.2 cm s^{-1}) was employed to successfully model process G/G′ which confirms this process is a one electron reduction process.

Aqueous H_2SO_4 Electrolyte. The presence of K^+ affects the decatungstosilicate framework reduction process even more strongly in the 0.05 M H_2SO_4 medium than in 0.1 M HCl (Figure 12). In 0.05 M H_2SO_4 containing 0.25 M K_2SO_4, process G/G′ ($E^{o\prime}$ = −0.272 V) and H/H′ ($E^{o\prime}$ = −0.528 V)

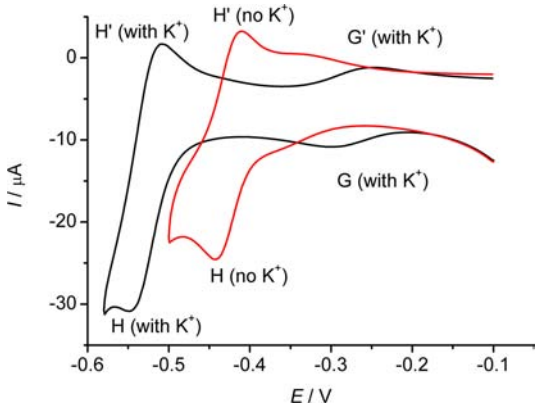

Figure 12. DC cyclic voltammograms for the polyoxometalate framework obtained at a glassy carbon electrode for 0.7 mM Rb_8K_2-**1**(0) in 0.05 M H_2SO_4 aqueous electrolyte solution in the presence (black solid line) and absence (red solid line) of 0.25 M K_2SO_4 at a scan rate of 0.025 V s^{-1}.

dx.doi.org/10.1021/ic301370y | *Inorg. Chem.* 2012, 51, 11521−11532

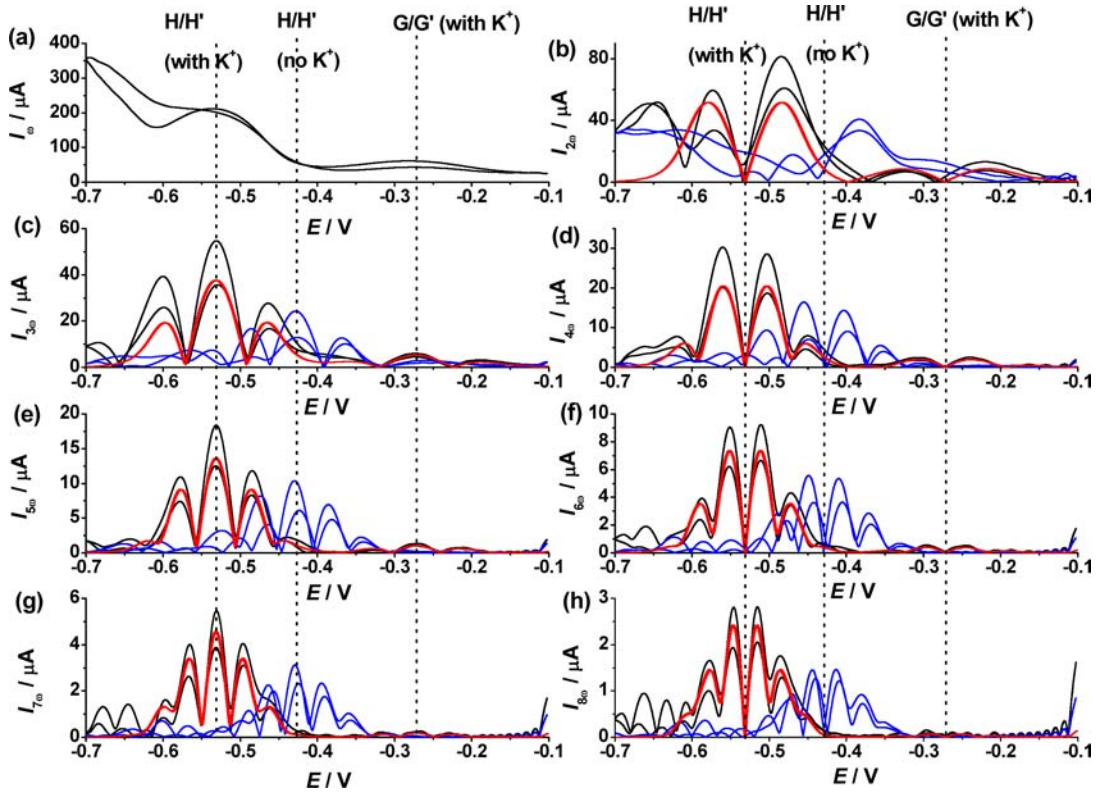

Figure 13. FT ac cyclic fundamental (a) to eighth (h) harmonic voltammetric component for the polyoxometalate framework obtained at a glassy carbon electrode for 0.7 mM Rb_8K_2-**1**(0) in 0.05 M H_2SO_4 aqueous electrolyte solution in the presence (black solid line) and absence (blue solid line, only second to sixth harmonics are shown in this case) of 0.25 M K_2SO_4. E_{start} = −0.10 V, E_{switch} = −0.70 V, E_{final} = −0.10 V, f = 9.02 Hz, ΔE = 0.08 V, ν = 0.0894 V s^{-1}. Reversible potentials associated with each process are designated by a reference line estimated from dc cyclic voltammogram. Simulation (red solid line) parameters for second (b) to eighth (h) ac harmonics are as experimental parameters, with $E^{o\prime}_{G/G'}$ = −0.272 V, $E^{o\prime}_{H/H'}(1)$ = −0.531 V, $E^{o\prime}_{H/H'}(2)$ = −0.531 V, $E^{o\prime}_{H/H'}(3)$ = −0.531 V, $E^{o}_{H/H'}(4)$ = −0.531 V, all with $k^{o\prime}$ = 1.0 cm s^{-1}, R_u= 80 Ω, C_{dl} = 60 μF cm^{-2}, α = 0.5, D = 1.80 × 10^{-6} cm^2 s^{-1}. For all processes, n = 1, where H/H′ is considered to have undergone four sequential electron transfers.

are well separated by 256 mV. The peak current for process H/H′ is many times greater than that of G/G′, again indicating that it represents an overall multielectron transfer process. RDE voltammograms were studied using rotation rates in the range of 52−314 rad s^{-1}. Comparisons of the I_L values for processes G/G′ and H/H′ with those for the well resolved one-electron transfer processes C/C′ and D/D′ provide estimates of n = 1.1 (±0.2) and 4.1 (±0.2) for processes G/G′ and H/H′, respectively. In the absence of a proton source or at high pH, a series of resolved one-electron reduction processes would be expected for the decatungstosilicate framework.[17] However, when the acidity of the medium increases, particularly processes at more negative potentials shift to more positive values and merge at sufficiently low pH because of the increasing importance proton-coupling to electron transfer.

The ac voltammetric results (Figure 13) are consistent with the dc ones. In 0.05 M H_2SO_4 containing 0.25 M K_2SO_4, the current magnitudes of second and higher harmonics are about double those obtained in the 0.1 M HCl medium in the presence of 0.5 M KCl, which again implies that the apparent electron transfer rate is faster in H_2SO_4 medium. In the absence of K^+, the current magnitudes for the second and higher harmonics are about half those obtained in the presence of K^+, indicating slower electron transfer kinetics. The reversible potential for process H/H′ is about 100 mV more positive in H_2SO_4 medium when K^+ is absent, which indicates substantial ion-pairing with K^+. Simulations based on a one electron transfer for process G/G′, and four sequential electron transfers processes again mimic well the experimental data for all ac harmonics with $k^{o\prime} \geq$ 1.0 cm s^{-1}, and hence faster than the value of 0.2 cm s^{-1} employed to simulate data in HCl medium. Thus, both dc and ac results are consistent with electron transfer kinetics of processes G/G′ and H/H′ being faster in H_2SO_4 than in HCl. The difference in $E^{o\prime}$ for process H/H′ in the presence or absence of K^+ is much larger in H_2SO_4 (about 100 mV) than in HCl medium (about 50 mV). This could be because of a combined effect of pH and ion-pairing with K^+.

■ CONCLUSIONS

Several electroanalytical methods have been employed to elucidate the details of the redox chemistry of Rb_8K_2-**1**(0) in acidic media. It is evident that the electrochemistry is affected by the presence of protons and potassium ions in both thermodynamic and kinetic senses. Protonation of the Ru-core changes the reaction thermodynamics while the potassium cation creates a faster and dominants electron transfer pathway. Via the choice of a suitable medium and use of the FT-ac voltammetric technique, the third and fourth $Ru^{IV/V}$ processes predicted to exist in previous work, and likely to be relevant in water oxidation catalysis, are revealed. The capability of resolving underlying faradaic processes from the solvent limit is clearly an advantage of this method.

dx.doi.org/10.1021/ic301370y | *Inorg. Chem.* 2012, 51, 11521−11532

AUTHOR INFORMATION

Corresponding Author

*E-mail: jie.zhang@monash.edu (J.Z.), alan.bond@monash.edu (A.M.B.), iguelet@emory.edu (Y.V.G.).

Notes

The authors declare no competing financial interest.

ACKNOWLEDGMENTS

Fourier transform simulation package (MECSim) used in this study was developed by Dr Gareth Kennedy. A.F.M. acknowledges the award from the EMBARK initiative scholarship scheme. Financial support from the Australian Research Council and from the U.S. National Science Foundation Grant CHE-0911610 is also gratefully acknowledged.

REFERENCES

(1) Vougioukalakis, G. C.; Grubbs, R. H. *Chem. Rev.* **2010**, *110*, 1746.
(2) Cook, T. R.; Dogutan, D. K.; Reece, S. Y.; Surendranath, Y.; Teets, T. S.; Nocera, D. G. *Chem. Rev.* **2010**, *110*, 6474.
(3) Gersten, S. W.; Samuels, G. J.; Meyer, T. J. *J. Am. Chem. Soc.* **1982**, *104*, 4029.
(4) Ruettinger, W.; Dismukes, G. C. *Chem. Rev.* **1997**, *97*, 1.
(5) Limburg, J.; Vrettos, J. S.; Liable-Sands, L. M.; Rheingold, A. L.; Crabtree, R. H.; Brudvig, G. W. *Science* **1999**, *283*, 1524.
(6) Liu, F.; Cardolaccia, T.; Hornstein, B. J.; Schoonover, T. R.; Meyer, T. J. *J. Am. Chem. Soc.* **2007**, *129*, 2446.
(7) Geletii, Y. V.; Botar, B.; Kögerler, P. K.; Hillesheim, D. A.; Musaev, G. G.; Hill, C. L. *Angew. Chem., Int. Ed.* **2008**, *47*, 3896.
(8) Geletii, Y. V.; Besson, C.; Hou, Y.; Yin, Q.; Musaev, D. G.; Quiñonero, D. Q.; Cao, R.; Hardcastle, K. I.; Proust, A.; Kögerler, P.; Hill, C. L. *J. Am. Chem. Soc.* **2009**, *131*, 17360.
(9) Sartorel, A.; Carraro, M.; Scorrano, G.; De Zorzi, R.; Geremia, S.; McDaniel, N. D.; Bernhard, S.; Bonchio, M. *J. Am. Chem. Soc.* **2008**, *130*, 5006.
(10) Sartorel, A.; Miro, P.; Salvadori, E.; Romain, S.; Carraro, M.; Scorrano, G.; Valentin, M. D.; Llobet, A.; Bo, C.; Bonchio, M. *J. Am. Chem. Soc.* **2009**, *131*, 16051.
(11) Walter, M. G.; Warren, E. L.; McKone, J. R.; Boettcher, S. W.; Mi, Q.; Santori, E. A.; Lewis, N. S. *Chem. Rev.* **2010**, *110*, 6446.
(12) Pope, M. T. *Heteropoly and Isopoly Oxometalates*; Springer-Verlag: Berlin, Germany, 1983.
(13) Sadakane, M.; Steckhan, E. *Chem. Rev.* **1998**, *98*, 219.
(14) Hill, C. L. In *Comprehensive Coordination Chemistry II*; McCleverty, J. A., Meyer., T. J., Eds.; Elsevier: Amsterdam, The Netherlands, 2004; Vol. *4*.
(15) Pope, M. T. In *Comprehensive Coordination Chemistry II*; McCleverty, J. A., Meyer., T. J., Eds.; Elsevier: Amsterdam, The Netherlands, 2004; Vol. *4*.
(16) Zhang, J.; Bond, A. M.; MacFarlane, D. R.; Forsyth, S. A.; Pringle, J. M.; Mariotti, A. W. A.; Glowinski, A. F.; Wedd, A. G. *Inorg. Chem.* **2005**, *44*, 5123.
(17) Grigoriev, V. A.; Cheng, D.; Hill, C. L.; Weinstock, I. A. *J. Am. Chem. Soc* **2001**, *123*, 5292.
(18) Guo, S.-X.; Mariotti, A. W. A.; Schlipf, C.; Bond, A. M.; Wedd, A. G. *Inorg. Chem.* **2006**, *45*, 8563.
(19) Zhang, J.; Bond, A. M.; Richardt, P. J. S.; Wedd, A. G. *Inorg. Chem.* **2004**, *43*, 8263.
(20) Czap, A.; Neuman, N. I.; Swaddle, T. W. *Inorg. Chem.* **2006**, *45*, 9518.
(21) Bond, A. M.; Noel, W. F.; Guo, S.-X.; Zhang, J.; Elton, D. M. *Anal. Chem.* **2005**, *77*, 186.
(22) Guo, S.-X.; Zhang, J.; Elton, D. M.; Bond, A. M. *Anal. Chem.* **2004**, *76*, 166.
(23) Lee, C. Y.; Fleming, B. D.; Zhang, J.; Guo, S.-X.; Elton, D. M.; Bond, A. M. *Anal. Chim. Acta* **2009**, *652*, 205.
(24) Fleming, B. D.; Zhang, J.; Elton, D. M.; Bond, A. M. *Anal. Chem.* **2007**, *79*, 6515.
(25) Lee, C. Y.; Bond, A. M. *Langmuir* **2010**, *26*, 16155.
(26) Zhang, J.; Guo, S.-X.; Bond, A. M.; Marken, F. *Anal. Chem.* **2004**, *76*, 3619.
(27) Zhang, J.; Guo, S.-X.; Bond, A. M. *Anal. Chem.* **2007**, *79*, 2276.
(28) Ma, H.; Shi, S.; Zhang, Z.; Pang, H.; Zhang, Y. *J. Electroanal. Chem.* **2010**, *648*, 128.
(29) Lee, C. Y.; Bullock, J. P.; Kennedy, G. P.; Bond, A. M. *J. Phys. Chem. A* **2010**, *114*, 10122.
(30) Bard, A. J. Faulkner, L. R. *Electrochemical methods: fundamentals and applications*, 2nd ed.; Wiley: New York, 2001.
(31) Swaddle, T. W. *Chem. Rev.* **2005**, *105*, 2573.
(32) Dunsch, L.; Inzelt, G.; Horanyi, G.; Lubert, K.-H. *Isotopenpraxis* **1990**, *26*, 343−346.
(33) Fuoss, R. M. *J. Am. Chem. Soc.* **1958**, *80*, 5059.
(34) Snir, O.; Wang, Y.; Tuckerman, M. E.; Geletii, Y. V.; Weinstock, I. A. *J. Am. Chem. Soc.* **2010**, *132*, 11678.
(35) Guo, S.-X.; Mariotti, A. W. A.; Schlipf, C.; Bond, A. M.; Wedd, A. G. *J. Electroanal. Chem.* **2006**, *591*, 7.
(36) Guo, S.-X.; Feldberg, S. W.; Bond, A. M.; Callahan, D. L.; Richardt, P. J. S.; Wedd, A. G. *J. Phys. Chem. B* **2005**, *109*, 20641.